Tacripyrines, the First Tacrine−Dihydropyridine Hybrids, as Multitarget-Directed Ligands for the Treatment of Alzheimer's Disease

José Marco-Contelles,*[,△] Rafael León,[△,†,‡] Cristóbal de los Ríos,[△,†,‡] Abdelouahid Samadi,[△] Manuela Bartolini,[§] Vincenza Andrisano,[§] Oscar Huertas,[||] Xavier Barril,[⊥] F. Javier Luque,[||] María I. Rodríguez-Franco,[#] Beatriz López,[#] Manuela G. López,[†,‡] Antonio G. García,[†,‡,▽] María do Carmo Carreiras,[○] and Mercedes Villarroya[†,‡]

Laboratorio de Radicales Libres (IQOG, CSIC), C/Juan de la Cierva 3, 28006 Madrid, Spain, Laboratorio de Radicales Libres (IQOG, CSIC), C/Juan de la Cierva 3, 28006-Madrid, Spain, Instituto Teófilo Hernando, C/Arzobispo Morcillo 4, 28029 Madrid, Spain, Departamento de Farmacología y Terapéutica, Facultad de Medicina, Universidad Autónoma de Madrid, C/Arzobispo Morcillo 4, 28029 Madrid, Spain, Department of Pharmaceutical Sciences, Alma Mater Studiorum, University of Bologna, Via Belmeloro 6, 40126 Bologna, Italy, Department de Fisicoquímica and Institut de Biomedicina (IBUB), Facultat de Farmàcia, Universitat de Barcelona, Avenida Diagonal 643, 08028 Barcelona, Spain, Institució Catalana de Recerca i Estudis Avançats (ICREA), Instituto de Química Médica (CSIC), C/Juan de la Cierva 3, 28006 Madrid, Spain, Servicio de Farmacología Clínica, Hospital Universitario de la Princesa, C/Diego de León 62, 28006 Madrid, Spain, iMEd.UL, Research Institute for Medicines and Pharmaceutical Sciences, Faculdade de Farmácia da Universidade de Lisboa, Av. Forças Armadas, 1600-083, Lisboa, Portugal

Received October 14, 2008

Tacripyrines (**1**−**14**) have been designed by combining an AChE inhibitor (tacrine) with a calcium antagonist such as nimodipine and are targeted to develop a multitarget therapeutic strategy to confront AD. Tacripyrines are selective and potent AChE inhibitors in the nanomolar range. The mixed type inhibition of hAChE activity of compound **11** (IC_{50} 105 ± 15 nM) is associated to a 30.7 ± 8.6% inhibition of the proaggregating action of AChE on the Aβ and a moderate inhibition of Aβ self-aggregation (34.9 ± 5.4%). Molecular modeling indicates that binding of compound **11** to the AChE PAS mainly involves the (*R*)-**11** enantiomer, which also agrees with the noncompetitive inhibition mechanism exhibited by *p*-methoxytacripyrine **11**. Tacripyrines are neuroprotective agents, show moderate Ca^{2+} channel blocking effect, and cross the blood−brain barrier, emerging as lead candidates for treating AD.

Introduction

Alzheimer's disease (AD) is an age-related neurodegenerative process characterized by progressive memory loss, decline in language skills, and other cognitive impairments.[1] Although the etiology of AD is not well-known, several factors such as amyloid-β (Aβ)[2] deposits, τ-protein aggregation, oxidative stress, or low levels of acetylcholine[3] are thought to play significant roles in the pathophysiology of the disease.[4] In spite of the enormous research effort, an efficient strategy for designing new drugs for the treatment of AD is still lacking.[a]

The cholinergic theory[1] suggests that the selective loss of cholinergic neurons in AD results in a deficit of acetylcholine (ACh) in specific regions of the brain that mediate learning and memory functions.[5] Consequently, there are four FDA-approved drugs (tacrine, donepezil, galantamine, and rivastigmine) that improve AD symptoms by inhibiting acetylcholinesterase (AChE), i.e., the enzyme responsible for the hydrolysis of ACh, thereby raising the levels of ACh in the synaptic cleft.[6] Recently, a renewed interest for AChE inhibitors (AChEI) has been stimulated by the potential role of AChE in accelerating the formation of amyloid fibrils in the brain and forming stable complexes with Aβ.[7] This role involves the peripheral anionic binding site (PAS) of AChE, as noted by the fact that propidium iodide, which binds to the PAS, affects the Aβ aggregation in vitro, whereas active-site inhibitors have no similar effect.[8]

The multifactorial nature of AD supports the most current innovative therapeutic approach based on the "one molecule, multiple targets" paradigm.[9−13] The multitarget approach[14] includes novel tacrine−melatonin hybrids,[15] dual inhibitors of AChE and monoamine oxidase[16] or serotonin transporters,[17] potent cholinesterase inhibitors with antioxidant and neuroprotective properties,[18] gallamine-tacrine hybrids binding at cholinesterases and M_2 muscarinic receptors,[19] or NO-donor−tacrine hybrids as hepatoprotective anti-Alzheimer drugs.[20]

It is known that Ca^{2+} overload is the main factor that triggers the processes leading to cell death. Thus, it has been shown that calcium dysfunction, involved in the pathogenesis of AD, augments Aβ formation and τ hyperphosphorylation.[21,22] Moreover, calcium entry through L-type Ca^{2+} channels (Cav 1.1−1.4) causes both calcium overload and mitochondrial disruption, which leads to the activation of the apoptotic cascade and cell death.[23] Hence, blocking the entrance of Ca^{2+} through this specific subtype of Ca^{2+} channel could be valuable to prevent cell death. In fact, nimodipine, a neuronal L-type Ca^{2+} channel blocker, protects neurons from death evoked by focal cerebral ischemia.[24]

* To whom correspondence should be addressed. Phone: +34-91-5622900. Fax: +34-91-5644853. E-mail: iqoc21@iqog.csic.es.

△ Laboratorio de Radicales Libres (IQOG, CSIC), Madrid, Spain.

† Instituto Teófilo Hernando.

‡ Departamento de Farmacología y Terapéutica, Universidad Autónoma de Madrid.

§ Department of Pharmaceutical Sciences, University of Bologna.

|| Department de Fisicoquímica and Institut de Biomedicina (IBUB), Universitat de Barcelona.

⊥ Institució Catalana de Recerca i Estudis Avançats (ICREA), Universitat de Barcelona.

Instituto de Química Médica (CSIC).

▽ Servicio de Farmacología Clínica, Hospital Universitario de la Princesa.

○ iMEd.UL, Research Institute for Medicines and Pharmaceutical Sciences, Universidade de Lisboa.

[a] Abbreviations: AD, Alzheimer's disease; ACh, acetylcholine; AChE, acetylcholinesterase; Aβ, β-amyloid peptide; BuChE, butyrylcholinesterase; AChEI, acetylcholinesterase inhibitors; hAChE, human acetylcholinesterase; Ee, *Electrophorus electricus*; BBB, blood−brain barrier; LDH, lactic dehydrogenase; VDCC, voltage-dependent Ca^{2+} channels; DHP, dihydropyridines; PAS, peripheral anionic site; PAMPA, parallel artificial membrane permeation assay.

10.1021/jm801292b CCC: $40.75 © 2009 American Chemical Society
Published on Web 04/17/2009

Chart 1. Tacripyrines **1**−**14** Based on the Juxtaposition of an AChEI (Tacrine) and a 1,4-DHP (Nimodipine)

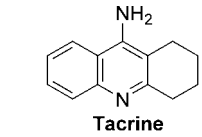

Tacrine

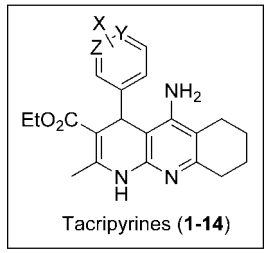

Tacripyrines (**1-14**)

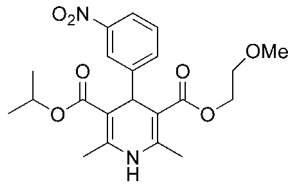

Nimodipine

Because 1,4-dihydropyridines (DHPs) are compounds that selectively block L-type voltage-dependent Ca^{2+} channels (VDCC), hybrid molecules that combine an AChEI and a DHP, such as tacrine and nimodipine (Chart 1), might represent a promising approach to the treatment of AD. Support to this therapeutic strategy comes from the fact that bis(7)-tacrine attenuates β-amyloid neuronal apoptosis by regulating L-type calcium channels.[25] Besides inhibition of AChE and blockade of VDCC, compounds able to prevent the oxidative stress might have increased therapeutic value because oxidative damage precedes the appearance of other pathological hallmarks of AD.[26−28]

On the basis of the preceding considerations, a preliminary study on the synthesis and biological evaluation of tacripyrines allowed us to conclude that these compounds are promising for further development as new drugs for the treatment of AD.[29] In this context, coupled to the simple synthetic schemes that yield multigram quantities of tacripyrines, new compounds have been synthesized in order to provide a broader structure−activity (AChE/BuChE) relationship (SAR), and new studies are now been incorporated describing the inhibition mechanism of AChE, the inhibition of the AChE-induced Aβ aggregation, as well as the inhibition of the self-aggregation of Aβ, molecular modeling on the active centers, the effect of these compounds on the regulation of the cytosolic calcium concentration, their neuroprotective properties against different cytotoxic *stimuli*, and finally studies directed to evaluate the ability of these compounds to cross the blood−brain barrier (BBB).

Results and Discussion

Chemistry. The synthesis of tacripyrines **1**−**14** ["ethyl ester of 5-amino-4-(hetero)aryl-1,4,6,7,8,9-hexahydro-2-methylbenzo[*b*][1,8]naphthyridine-3-carboxylic acid"] was easily achieved by reaction of the readily available ethyl esters of 3-*oxo*-2-(arylmethylene)-butanoic acids (**15**−**28**),[30−38] with 3,3-diaminoacrylonitrile (**29**),[39] prepared in situ from ethyl cyanoacetimidate hydrochloride (**30**)[40] (Scheme 1). The resulting ethyl esters of (±)-6-amino-4-aryl-5-cyano-2-methyl-1,4-dihydropyridine-3-carboxylic acids (**31**−**44**) were isolated from moderate to good chemical yields. In this work, we have described the synthesis of 3-*oxo*-2-(4′-biphenylmethylene)-butanoic acid (**22**) for the first time, and only compound **31** has been previously described by Troschütz.[41] Next, Friedländer reaction[42] between the β-enaminonitriles **31**−**44** and cyclohexanone, under standard conditions ($AlCl_3$, 1,2-dichloroethane, under reflux)[43] provided the desired target molecules (Scheme 1).

Compounds **1**−**14** are racemic hexahydrobenzo[*b*][1,8]naphthyridines substituted at C-4 by an aromatic ring incorporating different types of substituents, or by a 3′-(4′)pyridyl ring system. These molecules have been conveniently characterized by their analytical and NMR spectroscopic data (see Supporting Information).

Biology. AChE/BuChE Inhibitory Activity. Tacripyrines **1**−**14** were evaluated as inhibitors of AChE from *Electrophorus electricus* (Ee) following Rappaport's method,[44] as well as inhibitors of AChE/BuChE from human serum according to Ellman's protocol.[45] Most of the tacripyrines were more potent inhibitors of EeAChE, at nanomolar level, than tacrine, which was used as reference (Table 1). Compounds **3**, **4**, **6**, and **14**, bearing strong electron-withdrawing groups at C2′ or C4′ (2′-CF_3, 2′-NO_2, 4′-NO_2, 4′-pyridyl) had the lowest EeAChE inhibitory potency (IC_{50} values >200 nM). However, **4** and **6** were the only compounds able to inhibit hBuChE (IC_{50} values of 4.8 and 34.4 μM, respectively). Conversely, compounds **10**/**11** and **2**/**13**, bearing electron-donating (3′-MeO, 4′-MeO) or electron-withdrawing (4′-F, 3′-pyridyl) groups, respectively, had the best EeAChE inhibitory potencies, besides high hBuChE/EeAChE selectivity. Compound **5**, which has a nitro group at C3′, showed better EeAChE inhibition than its isomers **4** and **6**, with the nitro group located at C2′ or C4′, respectively. In general, compounds with a substituent at C2′ position were the poorest EeAChE inhibitors. Regardless of the electronic effect of the functional group, substituents at C4′ were well accepted for the inhibitory activity, except for the nitro-substituted compound **6**.

Inhibition experiments using human serum AChE (hAChE) provided results similar to those found with EeAChE. The inhibition of hAChE by compounds **1**−**14** was generally somewhat less potent than that found for EeAChE, but the selectivity for AChE was preserved (Table 1). Compounds **10** and **12** were the most potent hAChE inhibitors, whereas the inhibitory potency of **11** and **13** was slightly weakened relative to EeAChE. Overall, compounds **8** and **10**−**12**, whose inhibitory activity varies only by a factor of 2, are among the most potent inhibitors of hAChE (IC_{50} values ranging from 45 to 105 nM). Finally, comparing with tacrine, the reference compound, tacripyrines **8** and **10**−**12**, proved more potent, regardless of the AChE used, and selective for hBuChE.

To sum up, on going from tacrine to our new tacripyrines, the AChE inhibitory activity is potentiated, while BuChE inhibition dramatically drops, giving a new family of potent and selective AChE inhibitors. Accordingly, they should contribute to activate central cholinergic transmission, while it is plausible that these compounds are devoid of the side effects related to nonselective cholinesterase inhibitors.[46]

Kinetic Study of AChE Inhibition. The mechanism of inhibition of hAChE was investigated using *p*-methoxytacripyrine **11**, one of the most potent EeAChE inhibitors (see above). The inhibitory constant, K_i, was determined from the analysis of Lineweaver−Burk plots, which show both increasing slopes (lower V_{max}) and intercepts (higher K_m) with increasing inhibitor

Scheme 1. Synthesis of Tacripyrines (**1**−**14**)

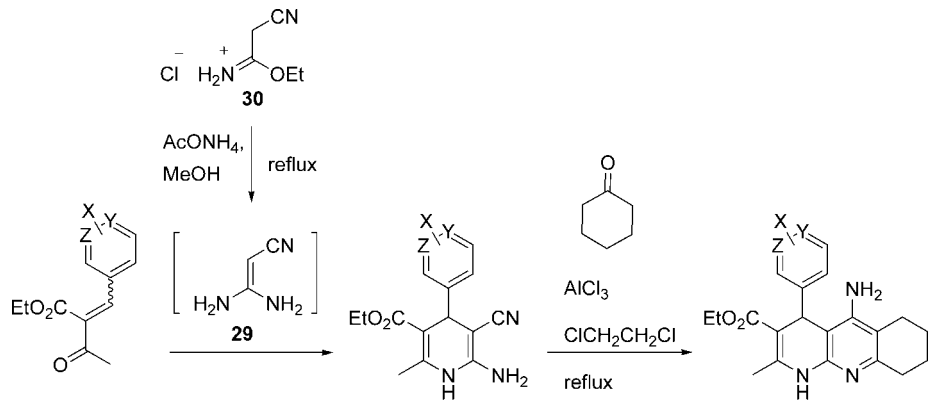

15 X= H, Y, Z= CH	**31** (80%)	**1** (96%)
16 X= 4'-F, Y= C, Z= CH	**32** (78%)	**2** (97%)
17 X= 2'-CF_3, Y, Z= CH	**33** (43%)	**3** (79%)
18 X= 2'-NO_2, Y, Z= CH	**34** (38%)	**4** (93%)
19 X= 3'-NO_2, Y, Z= CH	**35** (90%)	**5** (95%)
20 X= 4'-NO_2, Y= C, Z= CH	**36** (67%)	**6** (94%)
21 X= 4'-Me, Y= C, Z= CH	**37** (65%)	**7** (92%)
22 X= 4'-C_6H_5, Y= C, Z= CH	**38** (60%)	**8** (71%)
23 X= 2'-OMe, Y, Z= CH	**39** (32%)	**9** (64%)
24 X= 3'-OMe, Y, Z= CH	**40** (65%)	**10** (95%)
25 X= 4'-OMe, Y= C, Z= CH	**41** (74%)	**11** (51%)
26 X= 3', 4'-di-OMe, Y= C, Z= CH	**42** (77%)	**12** (94%)
27 X= H, Y= CH, Z= N	**43** (66%)	**13** (71%)
28 X= H, Y= N, Z= CH	**44** (85%)	**14** (90%)

Table 1. Inhibition of AChE from *Electrophorus electricus* (EeAChE), Human AChE (hAChE), and Human BuChE (hBuChE) by Tacripyrines **1**−**14**

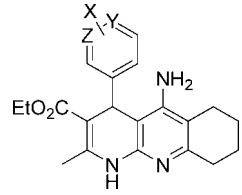

	X, Y, Z	IC_{50} (nM)[a] EeAChE[b]	IC_{50} (nM)[a] hBuChE[c]	IC_{50} (nM)[a] hAChE[c]	Selectivity IC_{50} hBuChE/IC_{50} hAChE
Tacrine		180 ± 20	36 ± 4	147 ± 11	0.24
1	X = H, Y, Z = CH	80 ± 2	>100000	122 ± 21	>820
2	X = 4′-F, Y = C, Z = CH	52 ± 9	>100000	193 ± 31	>518
3	X = 2′-CF_3, Y, Z = CH	210 ± 3	>100000	226 ± 27	>442
4	X = 2′-NO_2, Y, Z = CH	304 ± 2	4800 ± 40	338 ± 13	14.2
5	X = 3′-NO_2, Y, Z = CH	110 ± 2	>100000	191 ± 29	>524
6	X = 4′-NO_2, Y = C, Z = CH	600 ± 7	34400 ± 110	309 ± 21	111
7	X = 4′-Me, Y = C, Z = CH	91 ± 4	>100000	169 ± 15	>592
8	X = 4′-C_6H_5, Y = C, Z = CH	90 ± 2	>100000	71 ± 4	>1408
9	X = 2′-OMe, Y, Z = CH	160 ± 6	>100000	234 ± 32	>427
10	X = 3′-OMe, Y, Z = CH	61 ± 9	>100000	58 ± 7	>1724
11	X = 4′-OMe, Y = C, Z = CH	45 ± 5	>100000	105 ± 15	>952
12	X = 3′, 4′-di-OMe, Y = C, Z = CH	103 ± 6	>100000	45 ± 2	>2222
13	X = H, Y = CH, Z = N	47 ± 2	>100000	158 ± 20	>633
14	X = H, Y = N, Z = CH	220 ± 2	>100000	223 ± 43	>448

[a] IC_{50} values are the mean ± SEM of at least three independent measurements. [b] From *Electrophorus electricus* (Ee). [c] From human serum.

concentration, indicating mixed type inhibition. The graphical analysis of steady-state inhibition data for **11** is shown in Figure 1. A K_i value of 109 ± 1 nM was estimated from the plots of the slope versus the concentration of **11**.

Effects on AChE-Induced Aβ_{40} Aggregation. The availability of a suitable test for the study of the AChE-mediated Aβ_{40} aggregation allowed us to verify whether compound **11**, endowed with a mixed inhibition mechanism, could affect the Aβ aggregation. The results confirmed that AChE inhibitor **11** was able to interfere with the pro-aggregating action of hAChE with an inhibitory effect (%) of 30.7 ± 8.6. It is noteworthy that the parent AChE inhibitor tacrine was unable to significantly inhibit the AChE-induced Aβ_{40} aggregation.[8] Moreover, *p*-methoxytacripyrine **11** resulted in being more potent than donepezil and as potent as 3-{4-[(benzylmethylamino)methyl]phenyl}-6,7-dimethoxy-2*H*-2-chromenone (AP2238)[47] in this

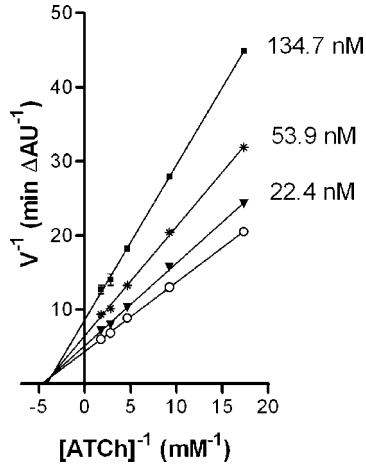

Figure 1. Steady-state inhibition of AChE hydrolysis of acetylthiocholine (ATCh) by **11**. Lineweaver−Burk reciprocal plots of initial velocity and substrate concentrations (0.058−0.578 mM) are presented. Lines were derived from a weighted least-squares analysis of the data points.

action. For the sake of completeness, it has to be mentioned that heterodimers of tacrine have been shown to be more potent in inhibiting the AChE-induced of Aβ_{40} aggregation.[8] It must be noticed that the assay is performed using much higher concentrations of hAChE and Aβ40 than those present in brain. Also, the concentration of inhibitor used is much higher (100 μM) than necessary to inhibit hAChE. However, the high hAChE concentration is necessary to accelerate the aggregation process up to a reasonable extent for analytical purposes; therefore to better estimate the obtained data, values should be normalized. Thus, if the inhibitor/AChE concentration ratio in both assays is taken into account, the resulting values are indeed of the same magnitude and, therefore, it would seem reasonable that similar amounts of a given inhibitor might afford both inhibitory activities. Moreover, the proof-of-concept of the therapeutic usefulness of the in vitro Aβ antiaggregating effect of dual binding site AChEIs has been recently obtained in in vivo studies with memoquin[9]

Effects on Aβ_{42} Self-Aggregation. Because Aβ_{42} is the most amyloidogenic isoform of β-amyloid, the ability of compound **11** to inhibit Aβ_{42} self-aggregation was also investigated. When tested in a 1:1 ratio with Aβ_{42} (50 μM), **11** gave rise to a 34.9 $\pm$ 5.4% of inhibition, whereas no significant inhibition was detected when the ratio [Aβ_{42}]/[inhibitor **11**] was 5/1. From these data, it can be stated that **11** is a weak inhibitor of Aβ_{42} self-aggregation. Its inhibitory action can be compared to that of resveratrol (30.0 $\pm$ 8.7% if tested at 50 μM). Moreover, it has to be noted that anti-Alzheimer drugs such as donepezil and tacrine were found to be inactive.

Molecular Modeling. The AChE binding mode of compound **11** was explored by means of docking and molecular dynamics (MD) studies (see Experimental Section). The reliability of the docking protocol was verified by examining the best poses predicted for tacrine and propidium by taking advantage of the known X-ray crystallographic binding mode of these compounds at the catalytic and peripheral sites, respectively, of AChE (data not shown),[48,49] thus giving confidence to the binding mode predicted for inhibitor **11**. Whereas compound **11** was not easily accommodated in the catalytic site, it was successfully docked in the PAS, which agrees with the noncompetitive inhibition mechanism exhibited by *p*-methoxytacripyrine **11**. According to the putative binding mode of the (*R*)-**11** enantiomer, the inhibitor is stacked against the indole ring of Trp286, while the

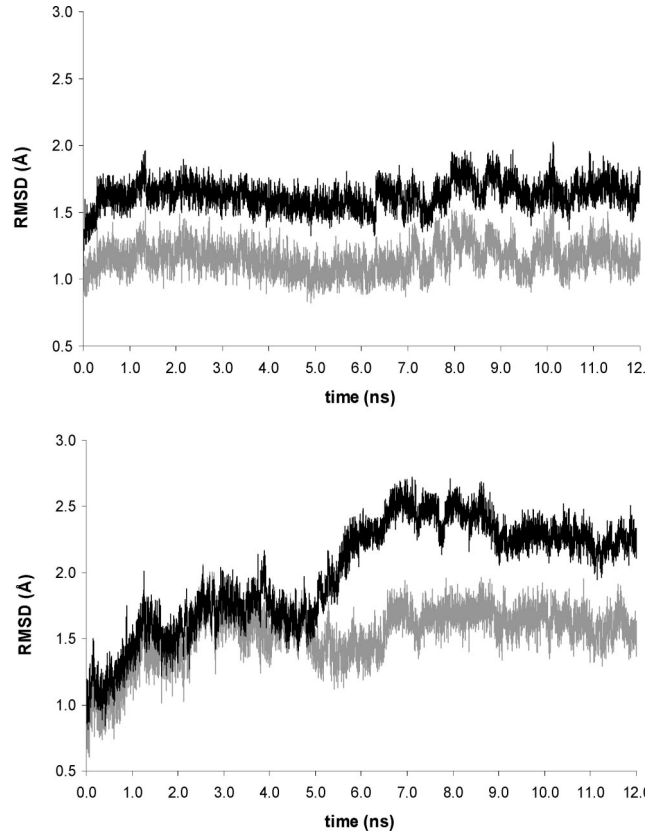

Figure 2. Time dependence of the root-mean square deviation (Å) of the backbone (gray) and all-heavy (black) atoms of the residues that define the PAS for the AChE complexes with (top) (*R*)- and (bottom) (*S*)-enantiomers of **11**.

NH group of the 1,8-naphthyridine unit is hydrogen-bonded to the hydroxyl group of Tyr72, which in turn is hydrogen-bonded to Asp74. The amino group is oriented toward Ser293, and the 4′-methoxybenzene unit is pointing toward the solvent, adopting a similar arrangement as the aliphatic chain containing the quaternary ammonium group in propidium, thus avoiding steric clashes with residues at the PAS. Compared to the enantiomer (*R*)-**11**, the 1,8-naphthyridine unit of the enantiomer (*S*)-**11** is rotated by ca. 180° along the short axis of the cyclic ring, which permits retention of the orientation of the 4′-methoxybenzene unit in the PAS, though at the expense of weakening the stacking with Trp286 because the ligand is located less deeply in the binding site (see Supporting Information).

To examine the relative binding affinity of the two enantiomers, a series of 12 ns MD simulations were run to explore the structural stability. Compared to the X-ray structure, the root-mean square deviation (rmsd) determined for the backbone and all-heavy atoms of the residues that define the PAS in the complex with the enantiomer (*R*)-**11** was around 1.1 and 1.5 Å, which indicates the structural stability of the complex along the trajectory (Figure 2). However, notably larger values were found for the rmsd of both the backbone (1.6 Å) and all-heavy atoms (2.3 Å) in the complex with the enantiomer (*S*)-**11**, suggesting that binding of the (*S*)-**11** to the PAS is associated with a large structural destabilization (Figure 2).

MM/PBSA computations were performed for the snapshots collected along the last 5 ns of the trajectories in order to examine the relative stabilities of the (*R*)-**11**−AChE and (*S*)-**11**−AChE complexes (Table 2). *The results indicate that binding of* **11** *to the AChE PAS mainly involves the (R)-enantiomer*. Thus, even though the electrostatic contribution due

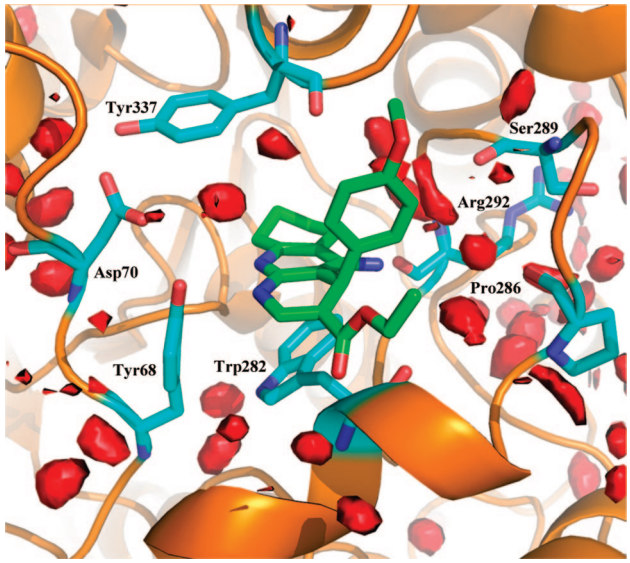

Figure 3. Representation of the binding mode of (*R*)-**11** in the PAS of AChE. Relevant residues of the PAS are shown in stick. The red contour denotes the presence of water at a density of two times that of pure bulk water.

Table 2. Relative Contributions to the Binding Affinity (kcal/mol) between (*R*)- and (*S*)-Enantiomers of **11** to AChE Determined from MM/PBSA Computations (Values Given Relative to the (*R*)-Enantiomer)

ε	ΔG_{MM}	ΔG^{sol}_{ele}	$\Delta G^{sol}_{nonpolar}$	$\Delta\Delta G_{binding}$
2	83.3	−80.9	1.1	3.6
4	38.4	−19.1	1.1	20.5

to the solvent reaction field favors the interaction with the (*S*)-enantiomer, this trend is compensated by the larger internal destabilization, which agrees with the structural distortion observed in the (*S*)-**11**−AChE complex (see above). In particular, the stacking with the indole ring of Trp286, which is a common feature observed experimentally[49−51] and from molecular modeling[52,53] studies for a variety of inhibitors interacting at the PAS, is lost in the binding mode of (*S*)-**11**.

The main features that mediate the binding of (*R*)-**11** to the PAS in the docking solution are preserved at the end of the MD simulation (see Figure 3). Besides the stacking with Trp286, it is worth noting the hydrogen-bond contact between the NH group of the 1,8-naphthyridine unit and the hydroxyl group of Tyr72 because this feature allows us to explain the 20-fold increase in the inhibitory potency observed between compounds **11** and the analogue obtained upon replacement of the NH moiety by O (IC_{50} of 870 nM in eeAChE).[54] Furthermore, it is also noteworthy the high density of water molecules found between the NH_2 group of the 1,8-naphthyridine unit and Ser293, suggesting that they also contribute to the binding at the PAS through water-mediated bridges. Finally, the lack of a tryptophan residue mimicking Trp286 in the peripheral site of hBuChE (replaced by Ala277), as well as the replacement of Tyr72 in hAChE by Asn68 in hBuChE, could also explain the large AChE/BuChE selectivity of these compounds.

Ca^{2+} Channel Blockade Activity of Tacripyrines. To study the multitarget activity of tacripyrines, we investigated the Ca^{2+} influx induced by K^+-depolarization in SH-SY5Y neuroblastoma cells, previously loaded with the fluorescent dye Fluo-4AM.

Fluo-4-loaded cells were incubated in the presence of compounds **1**−**14** (0.3 μM) for 10 min and then stimulated with a concentrated solution of KCl, so that the final K^+ concentration in the medium was 70 mM. In all experiments, we included a positive control such as nimodipine (0.3 μM), which caused 45.5% inhibition of K^+-evoked Ca^{2+} uptake.

Table 3. Effect of Compounds **1**−**14** on $[Ca^{2+}]_c$ Increase Elicited by 70 mM K^+ in SH-SY5Y Cells (% Inhibition with Respect to a Control without Any Drug)[a]

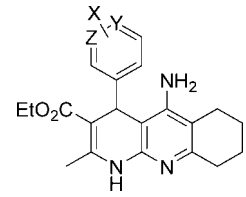

	X, Y, Z	% blockade in SH-SY5Y cells
nimodipine	−	45.5 ± 6.1***[d]
1	X = H, Y, Z = CH	36.64 ± 2.66*[b]
2	X = 4′-F, Y = C, Z = CH	22.22 ± 3.00 ns[e]
3	X = 2′-CF_3, Y, Z = CH	34.35 ± 2.12*[b]
4	X = 2′-NO_2, Y, Z = CH	32.65 ± 4.20**[c]
5	X = 3′-NO_2, Y, Z = CH	33.61 ± 5.10***[d]
6	X = 4′-NO_2, Y = C, Z = CH	33.65 ± 3.00***[d]
7	X = 4′-Me, Y = C, Z = CH	29.83 ± 3.98 ns
8	X = 4′-C_6H_5, Y = C, Z = CH	35.35 ± 4.94*[b]
9	X = 2′-OMe, Y, Z = CH	46.50 ± 4.44***[d]
10	X = 3′-OMe, Y, Z = CH	31.04 ± 4.10**[c]
11	X = 4′-OMe, Y = C, Z = CH	32.75 ± 2.50**[c]
12	X = 3′, 4′-di-OMe, Y = C, Z = CH	45.45 ± 5.70*[b]
13	X = H, Y = CH, Z = N	48.78 ± 2.30***[d]
14	X = H, Y = N, Z = CH	44.78 ± 5.60**[c]

[a] Data are expressed as means ± SEM of at least three different cultures in quadruplicate. [b] *$p < 0.05$. [c] **$p < 0.01$. [d] ***$p < 0.001$ with respect to $[Ca^{2+}]_c$ increase in control cells. All compounds were assayed at the concentration of 0.3 μM. [e] ns = not significant.

The calcium channel antagonist activities exhibited by compounds **1**−**14** are shown in Table 3. Most of the tested compounds promoted significant Ca^{2+} blockade, the most potent being hybrid **13**, whose activity (49% inhibition) was similar to that obtained with nimodipine (i.e., the reference compound used in this assays) at the same concentration. Tacripyrines **9**, **12**, and **14** also showed good blockade (>44% inhibition) regardless of the electronic nature of the substituents or the groups attached to the aromatic ring.

Neuroprotection. Prompted by the results obtained for compounds **1**−**14** as $[Ca^{2+}]_c$ blockers, their potential neuroprotective activity was investigated. For this purpose, we studied the effects of **1**−**14** on SH-SY5Y cells exposed for 24 h to a medium with a depolarizing concentration of KCl (70 mM), which induced Ca^{2+} overload and cell death. Drugs at a concentration of 0.3 μM were administered 24 h before incubation of the cells with high K^+ (70 mM; hypertonic) and maintained during the entire experiment. Thereafter, release of lactic dehydrogenase (LDH) was measured as a marker of cell death.[55]

As shown in Table 4, all compounds afforded a higher degree of neuroprotection compared to tacrine and within the same range relative to nimodipine. Only **4** did not show a statistically significant protection against Ca^{2+} overload. Tacripyrines **2**, **6**, and **11** were the most effective compounds with protection activities (%) of 48.8, 45.0, and 41.3, respectively. Again, it has to be highlighted that the electronic nature of the substituents in the aromatic ring does not seem to have a critical influence on the observed activities.

Antioxidant Activity. The antioxidant activity of **1**−**14** was evaluated at a concentration of 0.3 μM on SH-SY5Y neuroblastoma cells exposed to 60 μM H_2O_2 for 24 h.

The results shown in Table 5 indicate that tacripyrines protect much more efficiently against free radicals than the parent compounds, tacrine and nimodipine, which did not show any

Table 4. Effect of Tacripyrines **1**-**14** on SH-SY5Y Cells Viability Expressed as % LDH Released in the Presence of 70 mM K^{+a} and % Protection

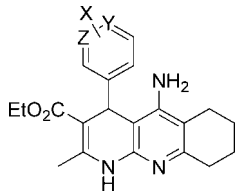

	X	LDH release (% of control)	% protection
tacrine		90.4 ± 4.1 ns[c]	13.4 ± 7.2
nimodipine		75.00 ± 2.24***[b]	35.93 ± 2.84
1	X = H, Y, Z = CH	75.02 ± 2.56***[b]	35.92 ± 3.53
2	X = 4′-F, Y = C, Z = CH	61.22 ± 2.10***[b]	48.79 ± 3.99
3	X = 2′-CF_3, Y, Z = CH	79.29 ± 1.64***[b]	29.79 ± 2.20
4	X = 2′-NO_2, Y, Z = CH	88.29 ± 2.99 ns	16.59 ± 4.18
5	X = 3′-NO_2, Y, Z = CH	77.87 ± 2.74***[b]	31.80 ± 3.81
6	X = 4′-NO_2, Y = C, Z = CH	63.91 ± 2.34***[b]	45.03 ± 4.02
7	X = 4′-Me, Y = C, Z = CH	72.43 ± 1.89***[b]	39.70 ± 2.47
8	X = 4′-C_6H_5, Y = C, Z = CH	81.50 ± 4.61**[b]	26.51 ± 6.59
9	X = 2′-OMe, Y, Z = CH	77.61 ± 1.66***[b]	32.23 ± 2.21
10	X = 3′-OMe, Y, Z = CH	68.96 ± 1.33***[b]	38.77 ± 3.43
11	X = 4′-OMe, Y = C, Z = CH	67.63 ± 2.24***[b]	41.30 ± 4.95
12	X = 3′,4′-di-OMe, Y = C, Z = CH	73.66 ± 1.84***[b]	37.89 ± 2.37
13	X = H, Y = CH, Z = N	75.77 ± 2.18***[b]	32.82 ± 4.90
14	X = H, Y = N, Z = CH	74.31 ± 1.48***[b]	37.11 ± 1.96

[a] Data are expressed as the means ± SEM of at least three different batches of cells in quadruplicate. LDH released was calculated for each individual experiment, considering 100% the extracellular LDH released in the presence of vehicle. To calculate % protection, LDH release was normalized as follows: in each individual quadruplicate experiment, the LDH release obtained in nontreated cells (basal) was subtracted from the LDH released upon 70 mM K^+ treatment and normalized to 100%, then that value was subtracted from 100. All the compounds were assayed at a concentration of 0.3 μM. [b] ***$p < 0.001$. [c] ns = not significant.

neuroprotective effect. Compounds **7**, **11**, **13**, and **14** exhibited neuroprotection values higher than 50%, whereas **2** and **8**−**10** elicited neuroprotection activities ranging from 44% to 48%. Thus, three of the most potent neuroprotectors in this assay (**2**, **7**, and **11**) also proved to be among the most efficient in the previous test (see Table 3).

In Vitro Blood−**Brain Barrier (BBB) Permeation Assay.** To evaluate the brain penetration of tacripyrines, we used a parallel artificial membrane permeation assay for blood−brain barrier (PAMPA-BBB), following in part the method described by Di et al.[56] that was successfully applied by us to different compounds[57,58] The in vitro permeabilities (P_e) of tacripyrines **1**−**14** and 18 commercial drugs through a lipid extract of porcine brain were determined (see Table 6). Assay validation was made by comparing the experimental permeability with the reported values of the commercial drugs, which showed a good correlation, P_e (exp) = 0.99 P_e (bibl) − 1.32 (r = 0.90). From this equation and taking into account the limits established by Di et al. for BBB permeation,[56] we established the ranges of permeability as (i) compounds of high BBB permeation (CNS+): P_e (10^{-6} cm s^{-1}) > 2.7, (ii) compounds of low BBB permeation (CNS−): P_e (10^{-6} cm s^{-1}) < 0.7, and (iii) compounds of uncertain BBB permeation (CNS±): 2.7 > P_e (10^{-6} cm s^{-1}) > 0.7. As it can be seen in Table 6, the assay showed that almost all tacripyrines could cross the BBB and reach their biological targets in the central nervous system. Only two compounds, **3** and **7**, showed uncertain brain permeation (CNS ±).

Conclusions

We have synthesized and evaluated a series of tacrine-DHP hybrids, named tacripyrines, which are potent and selective inhibitors of AChE and show potent neuroprotection activity.

Table 5. Effect of Tacripyrines **1**−**14** on SH-SY5Y Cells Viability Expressed as % LDH Released in the Presence of 60 μM H_2O_2[a] and % Protection

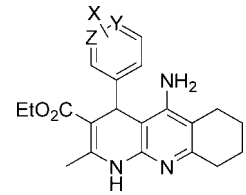

	X, Y, Z	LDH release (% of control)	% protection
catalase	−	18.93 ± 1.77***[b]	88.34 ± 2.80
tacrine	−	100.34 ± 3.37 ns[c]	0
nimodipine	−	75.42 ± 2.12***[b]	36.03 ± 2.82
1	X = H, Y, Z = CH	76.61 ± 1.83***[b]	30.60 ± 1.96
2	X = 4′-F, Y = C, Z = CH	64.17 ± 1.53***[b]	46.11 ± 2.02
3	X = 2′-CF_3, Y, Z = CH	71.72 ± 1.29***[b]	37.21 ± 1.27
4	X = 2′-NO_2, Y, Z = CH	71.91 ± 1.23***[b]	37.18 ± 1.61
5	X = 3′-NO_2, Y, Z = CH	77.19 ± 1.69***[b]	30.09 ± 2.18
6	X = 4′-NO_2, Y = C, Z = CH	72.43 ± 2.99***[b]	35.48 ± 3.78
7	X = 4′-Me, Y = C, Z = CH	59.60 ± 0.92***[b]	53.68 ± 1.62
8	X = 4′-C_6H_5, Y = C, Z = CH	62.24 ± 3.65***[b]	47.82 ± 4.06
9	X = 2′-OMe, Y, Z = CH	63.78 ± 1.35***[b]	48.23 ± 2.24
10	X = 3′-OMe, Y, Z = CH	65.14 ± 1.23***[b]	44.80 ± 1.53
11	X = 4′-OMe, Y = C, Z = CH	56.55 ± 1.94***[b]	55.78 ± 2.32
12	X = 3′, 4′-di-OMe, Y = C, Z = CH	77.42 ± 2.22***[b]	29.41 ± 2.43
13	X = H, Y = CH, Z = N	57.51 ± 2.25***[b]	54.38 ± 2.03
14	X = H, Y = N, Z = CH	60.32 ± 1.50***[b]	52.61 ± 2.01

[a] Data expressed as the means ± SEM of at least three different cultures in quadruplicate. LDH released was calculated for each individual experiment, considering 100% the extracellular LDH released in the presence of vehicle. To calculate % protection, LDH release was normalized as follows: in each individual quadruplicate experiment, the LDH release obtained in nontreated cells (basal) was subtracted from the LDH released upon 70 mM K^+ treatment and normalized to 100%, then that value was subtracted from 100. All the compounds were assayed at a concentration of 0.3 μM. [b] ***$p < 0.001$. [c] ns = not significant.

Table 6. Permeability (P_e 10^{-6} cm s^{-1}) in the PAMPA-BBB Assay of 18 Commercial Drugs and Tacripyrines **1**−**14**[a] (Predictive Penetration in the CNS)

commercial drugs	bibl[b]	exp[c]	compd	P_e (10^{-6} cm s^{-1})[c]	CNS prediction
testosterone	17.0	23.1 ± 0.1	**1**	12.6 ± 0.2	CNS+
verapamil	16.0	12.6 ± 0.2	**2**	9.6 ± 0.1	CNS+
imipramine	13.0	7.3 ± 0.2	**3**	1.4 ± 0.1	CNS±
desipramine	12.0	13.9 ± 0.1	**4**	8.6 ± 0.2	CNS+
astemizole	11.0	6.1 ± 0.2	**5**	7.0 ± 0.1	CNS+
progesterone	9.3	6.6 ± 0.5	**6**	5.8 ± 0.1	CNS+
promazine	8.8	7.7 ± 0.2	**7**	1.8 ± 0.1	CNS±
chlorpromazine	6.5	1.4 ± 0.2	**8**	nd[d]	
clonidine	5.3	4.2 ± 0.3	**9**	6.1 ± 0.1	CNS+
corticosterone	5.1	3.6 ± 0.3	**10**	5.5 ± 0.1	CNS+
piroxicam	2.5	0.4 ± 0.1	**11**	12.8 ± 0.2	CNS+
hydrocortisone	1.9	1.2 ± 0.2	**12**	9.4 ± 0.1	CNS+
caffeine	1.3	1.0 ± 0.1	**13**	7.2 ± 0.4	CNS+
aldosterone	1.2	0.6 ± 0.1	**14**	6.2 ± 0.1	CNS+
lomefloxacin	1.1	0.5 ± 0.1			
enoxacin	0.9	0.6 ± 0.2			
atenolol	0.8	0.03 ± 0.01			
ofloxacin	0.8	0.3 ± 0.01			

[a] Commercial drugs and tacripyrines were tested using a mixture of PBS:EtOH (80:20). [b] Taken from ref 56. [c] Data are expressed as the means ± standard deviation of three different experiments in quadruplicate. nd: not determined. [d] Permeability was not determined due to the poor solubility in PBS:EtOH (80:20).

A variety of substituted compounds have been easily prepared by simple, high-yielding protocols from readily available precursors. From the AChE inhibition results, we conclude that tacripyrines are potent AChE inhibitors regardless of the electronic nature of the substitution at C4, the best AChEI tacripyrine being compounds **8** and **10**−**12** on both EeAChE and hAChE. These hybrids were also devoid of hBuChE

inhibition activity, showing, therefore, an extremely high selectivity. Moreover, the mixed type inhibition of hAChE activity of compound **11**, one of the most potent derivatives, was associated to a 30.7 ± 8.6% inhibition of the proaggregating action of AChE on the β-amyloid peptide. Compound **11** was also a moderate inhibitor of β-amyloid self-aggregation (34.9 ± 5.4%). Molecular modeling results point out that AChE-inhibitor **11** is not easily accommodated in the catalytic site, but it can be successfully docked in the PAS, which agrees with the noncompetitive inhibition mechanism exhibited by **11**. In addition, the inhibitor (*R*)-**11** is stacked against the indole ring of Trp286, while the NH group of the 1,8-naphthyridine unit is hydrogen-bonded to the hydroxyl group of Tyr72, which in turn is hydrogen-bonded to Asp74. The amino group is oriented toward Ser293, and the 4′-methoxybenzene unit is pointing toward the solvent, adopting a similar arrangement as the aliphatic chain containing the quaternary ammonium group in propidium, thus avoiding steric clashes with residues at the PAS. Compared with the enantiomer (*S*)-**11**, the binding of this inhibitor in the AChE PAS mainly involves the (*R*)-**11** enantiomer.[59]

Most of the compounds blocked $[K^+]$-induced $[Ca^{2+}]_c$ increase in a statistically significant manner and induced a remarkable neuroprotective effect against both Ca^{2+} overload and oxidative stress. The fact that these compounds provide protection against two *stimuli* with different mechanisms of action (i.e., calcium overload and free radical generation) indicates that they could exert their effects on the apoptotic cell death cascade beyond the particular mechanism of each toxic agent. In particular, they might induce the expression of proteins implicated in cell survival, as demonstrated previously for a tacrine analogue.[54] These findings, in conjunction with the predicted ability to enter the central nervous system, indicate that tacripyrines can be considered as interesting new chemical entities with potential therapeutic application for AD patients.

Experimental Section

General Method for the Friedländer Reaction. Aluminum chloride (1.2−1.7 equiv) was suspended in dry 1,2-dichloroethane (10 mL) at rt under argon. The corresponding 4*H*-benzopyran (1 equiv) and cyclohexanone (1.2−1.7 equiv) were added. The reaction mixture was heated under reflux (10−24 h). When the reaction was over (TLC analysis), a mixture of THF/H_2O (1:1) was added at rt. An aqueous solution of sodium hydroxide (10%) was added dropwise to the mixture until the aqueous solution was basic. After stirring for 30 min, the mixture was extracted three times with dichloromethane. The organic layer was washed with brine, dried over anhydrous sodium sulfate, and filtered, and the solvent was evaporated. The resultant solid was purified by silica gel flash chromatography using methanol/dichloromethane mixtures as eluent to give pure compounds.

Ethyl Ester of 5-Amino-1,4,6,7,8,9-hexahydro-2-methyl-4-(2′-trifluoromethylphenyl)-drobenzo[*b*][1,8]naphthyridine-3-carboxylic Acid (3). Following the general method for the Friedländer synthesis, reaction of compound **33** (200 mg, 0.57 mmol) with $AlCl_3$ (113.05 mg, 0.85 mmol) and cyclohexanone (83.68 mg, 0.85 mmol), in $ClCH_2CH_2Cl$ (5 mL), after 6 h, gave product **3** (194 mg, 79%); mp 124−126 °C. IR (KBr) ν 3421,2934, 2862, 1688,1630, 1557, 1502, 1448, 1310, 1233 cm^{-1}. ^1H NMR (see Table 9, Supporting Information). ^{13}C NMR (see Table 10, Supporting Information). MS (API-ES+) *m*/*z*: $[M + 1]^+$ 432.1; $[2M + Na]^+$ 885.1. Anal. ($C_{23}H_{24}F_3N_3O_2$) C, H, N.

Ethyl Ester of 5-Amino-4-(4′-biphenyl)-1,4,6,7,8,9-hexahydro-2-methyl-benzo[*b*][1,8]naphthyridine-3-carboxylic Acid (8). Following the general method for the Friedländer synthesis, reaction of compound **38** (150 mg, 0.42 mmol) with $AlCl_3$ (125.7 mg, 0.63 mmol) and cyclohexanone (61.7 mg, 0.63 mmol), in $ClCH_2CH_2Cl$ (5 mL), after 7 h, gave product **8** (131.0 mg, 71%); mp 195−197 °C. IR (KBr) ν 3414, 3021, 2931, 2862, 1630, 1573, 1483, 1449, 1243 cm^{-1}. ^1H NMR (see Table 9, Supporting Information). ^{13}C NMR (see Table 10, Supporting Information). MS (API-ES+) *m*/*z*: $[M + 1]^+$ 440.2; $[2M + Na]^+$ 901.5. Anal. ($C_{28}H_{29}N_3O_2$) C, H, N.

Ethyl Ester of 5-Amino-4-(3′,4′-dimethoxyphenyl)-1,4,6,7,8,9-hexahydro-2-methyl-benzo[*b*][1,8]naphthyridine-3-carboxylic (12). Following the general method for the Friedländer synthesis, reaction of compound **42** (200 mg, 0.58 mmol) with $AlCl_3$ (105.8 mg, 0.87 mmol) and cyclohexanone (85.62 mg, 0.87 mmol), in $ClCH_2CH_2Cl$ (5 mL), after 4 h, gave product **12** (233.1 mg, 94%); mp 112−115 °C. IR (KBr) ν 3392, 2932, 1627, 1511, 1448, 1264, 1230 cm^{-1}. ^1H NMR (see Table 9, Supporting Information). ^{13}C NMR (see Table 10, Supporting Information)). MS (API-ES+) *m*/*z*: $[M + 1]^+$ 424.2. Anal. ($C_{24}H_{29}N_3O_4$) C, H, N.

Ethyl Ester of 5-Amino-1,4,6,7,8,9-hexahydro-2-methyl-4-(3′-pyridyl)benzo[*b*][1,8]naphthyridine-3-carboxylic Acid (13). Following the general method for the Friedländer synthesis, reaction of compound **43** (250 mg, 0.88 mmol) with $AlCl_3$ (175.56 mg, 1.32 mmol) and cyclohexanone (129.4 mg, 1.32 mmol), in $ClCH_2CH_2Cl$ (5 mL), after 6 h, gave product **13** (259 mg, 71%); mp 132−134 °C. IR (KBr) ν 3379, 3217, 3079, 2971, 2933, 2172, 1627, 1576, 1501, 1447, 1383 cm^{-1}. ^1H NMR (see Table 9, Supporting Information). ^{13}C NMR (see Table 10, Supporting Information). MS (API-ES+) *m*/*z*: $[M + 1]^+$ 365.2; $[2M + Na]^+$ 751.3. Anal. ($C_{23}H_{27}N_3O_3$) C, H, N.

Ethyl Ester of 5-Amino-1,4,6,7,8,9-hexahydro-2-methyl-4-(4′-pyridyl)benzo[*b*][1,8]naphthyridine-3-carboxylic Acid (14). Following the general method for the Friedländer synthesis, reaction of compound **44** (200 mg, 0.70 mmol) with $AlCl_3$ (139.65 mg, 1.05 mmol) and cyclohexanone (103.5 mg, 1.05 mmol), in $ClCH_2CH_2Cl$ (5 mL), after 15 h, gave product **14** (232 mg, 90%); mp 194−7 °C. IR (KBr) ν 3406, 2928, 2855, 1631, 1602, 1448, 1270 cm^{-1}. ^1H NMR (see Table 9, Supporting Information). ^{13}C NMR (see Table 10, Supporting Information). MS (API-ES+) *m*/*z*: $[M + 1]^+$ 365.2; $[M + Na]^+$ 387.1; $[2M + Na]^+$ 751.5. Anal. ($C_{21}H_{24}N_4O_2$) C, H, N.

Acknowledgment. J.M.C. thanks Dr. M[a]. Luz de la Puente (Analytical Technologies Department, Lilly SA), and Dr. M[a]. Angeles Martínez-Grau (Lilly SA) for the resolution of compound **11**. J.M.C. and also R.L. thank MEC for a fellowship (AP20020576) and B.L. thanks CSIC for a I3P Training Contract. The present work has been supported by Fundación Teófilo Hernando, MEC grants BFI2003-02722; SAF2006-08764-C02-01, SAF-2006-08540, SAF2006-1249, and CTQ2005-09365, CAM (S/SAL-0275-2006), ISCIII [Red RENEVAS (RD06/0026/1002)], CSIC-GRICES project (2007PT-13), and Fundación La Caixa (Barcelona, Spain).

Supporting Information Available: Experimental details for chemistry, spectroscopy [NMR data for intermediate (**32**-**44**) and target compounds (**1**, **2**, **4**−**6**, **7**, **9**−**11**)], elemental analyses for new intermediate (**32**−**44**) and target molecules (**1**−**14**), biology, modeling, including the best poses for the (*R*)- and (*S*)-enantiomers of **11** predicted from docking studies, and references cited therein. Chromatograms and experimental conditions for the chiral HPLC-mediated resolution of racemic *p*-methoxytacripyrine (**11**), ^1H NMR spectra, quiroptical properties, and the inhibition of AChE/BuChE, of the separated enantiomers (**A**)-**11** and (**B**)-**11**. This material is available free of charge via the Internet at http://pubs.acs.org.

References

(1) Goedert, M.; Spillantini, M. G. A century of Alzheimer's disease. *Science* **2006**, *314*, 777–781.
(2) Castro, A.; Martínez, A. Targeting beta-amyloid pathogenesis through acetylcholinesterase inhibitors. *Curr. Pharm. Des.* **2006**, *12*, 4377–4387.

(3) Cummings, J. L. Treatment of Alzheimer's disease: current and future therapeutic approaches. *Rev. Neurol. Dis.* **2004**, *1*, 60–69.
(4) Scarpini, E.; Scheltens, P.; Feldman, H. Treatment of Alzheimer's disease: current status and new perspectives. *Lancet Neurol.* **2003**, *2*, 539–547.
(5) Talesa, V. N. Acetylcholinesterase in Alzheimer's disease. *Mech. Ageing Dev.* **2001**, *122*, 1961–1969.
(6) Racchi, M.; Mazzucchelli, M.; Porrello, E.; Lanni, C.; Govoni, S. Acetylcholinesterase inhibitors: novel activities of old molecules. *Pharmacol. Res.* **2004**, *50*, 441–451.
(7) Inestrosa, N. C.; Álvarez, A.; Pérez, C. A.; Moreno, R. D.; Vicente, M.; Linker, C.; Casanueva, O. I.; Soto, C.; Garrido, J. Acetylcholinesterase accelerates assembly of amyloid-beta-peptides into Alzheimer's fibrils: possible role of the peripheral site of the enzyme. *Neuron* **1996**, *16*, 881–891.
(8) Bartolini, M.; Bertucci, C.; Cavrini, V.; Andrisano, V. beta-Amyloid aggregation induced by human acetylcholinesterase: inhibition studies. *Biochem. Pharmacol.* **2003**, *65*, 407–416.
(9) Cavalli, A.; Bolognesi, M. L.; Capsoni, S.; Andrisano, V.; Bartolini, M.; Margotti, E.; Cattaneo, A.; Recanatini, M.; Melchiorre, C. A small molecule targeting the multifactorial nature of Alzheimer's disease. *Angew. Chem., Int. Ed.* **2007**, *46*, 3689–3692.
(10) Muñoz-Torrero, D.; Camps, P. Dimeric and hybrid anti-Alzheimer drug candidates. *Curr. Med. Chem.* **2006**, *13*, 399–422.
(11) Savini, L.; Gaeta, A.; Fattorusso, C.; Catalanotti, B.; Campiani, G.; Chiasserini, L.; Pellerano, C.; Novellino, E.; McKissic, D.; Saxena, A. Specific targeting of acetylcholinesterase and butyrylcholinesterase recognition sites. Rational design of novel, selective, and highly potent cholinesterase inhibitors. *J. Med. Chem.* **2003**, *46*, 1–4.
(12) Decker, M. Homobivalent quinazolinimines as novel nanomolar inhibitors of cholinesterases with dirigible selectivity toward butyrylcholinesterase. *J. Med. Chem.* **2006**, *49*, 5411–5413.
(13) Carlier, P. R.; Chow, E. S.; Han, Y.; Liu, J.; El Yazal, J.; Pang, Y. P. Heterodimeric tacrine-based acetylcholinesterase inhibitors: investigating ligand−peripheral site interactions. *J. Med. Chem.* **1999**, *42*, 4225–4231.
(14) Cavalli, A.; Bolognesi, M. L.; Minarini, A.; Rosini, M.; Tumiatti, V.; Recanatini, M.; Melchiorre, C. Multi-target-directed ligands to combat neurodegenerative diseases. *J. Med. Chem.* **2008**, *51*, 347–372.
(15) Rodríguez-Franco, M. I.; Fernández-Bachiller, M. I.; Pérez, C.; Hernández-Ledesma, B.; Bartolomé, B. Novel tacrine-melatonin hybrids as dual-acting drugs for Alzheimer's disease with improved acetylcholinesterase inhibitory and antioxidant properties. *J. Med. Chem.* **2006**, *49*, 459–462.
(16) Sterling, J.; Herzig, Y.; Goren, T.; Finkelstein, N.; Lerner, D.; Goldenberg, W.; Miskolczi, I.; Molnar, S.; Rantal, F.; Tamas, T.; Toth, G.; Zagyva, A.; Zekany, A.; Finberg, J.; Lavian, G.; Gross, A.; Friedman, R.; Razin, M.; Huang, W.; Krais, B.; Chorev, M.; Youdim, M. B.; Weinstock, M. Novel dual inhibitors of AChE and MAO derived from hydroxy aminoindan and phenethylamine as potential treatment for Alzheimer's disease. *J. Med. Chem.* **2002**, *45*, 5260–5279.
(17) Toda, N.; Tago, K.; Marumoto, S.; Takami, K.; Ori, M.; Yamada, N.; Koyama, K.; Naruto, S.; Abe, K.; Yamazaki, R.; Hara, T.; Aoyagi, A.; Abe, Y.; Kaneko, T.; Kogen, H. A conformational restriction approach to the development of dual inhibitors of acetylcholinesterase and serotonin transporter as potential agents for Alzheimer's disease. *Bioorg. Med. Chem.* **2003**, *11*, 4389–4415.
(18) Rosini, M.; Antonello, A.; Cavalli, A.; Bolognesi, M. L.; Minarini, A.; Marucci, G.; Poggesi, E.; Leonardi, A.; Melchiorre, C. Prazosin-related compounds. Effect of transforming the piperazinylquinazoline moiety into an aminomethyltetrahydroacridine system on the affinity for alpha1-adrenoreceptors. *J. Med. Chem.* **2003**, *46*, 4895–4903.
(19) Elsinghorst, P. W.; Cieslik, J. S.; Mohr, K.; Tränkle, C.; Gütschow, M. First gallamine−tacrine hybrid: design and characterization at cholinesterases and the M2 muscarinic receptor. *J. Med. Chem.* **2007**, *50*, 5685–5695.
(20) Fang, L.; Appenroth, D.; Decker, M.; Kiehntopf, M.; Roegler, C.; Deufel, T.; Fleck, C.; Peng, S.; Zhang, Y.; Lehmann, J. Synthesis and biological evaluation of NO-donor-tacrine hybrids as hepatoprotective anti-Alzheimer drug candidates. *J. Med. Chem.* **2008**, *51*, 713–716.
(21) Kruman, I.; Guo, Q.; Mattson, M. P. Calcium and reactive oxygen species mediate staurosporine-induced mitochondrial dysfunction and apoptosis in PC12 cells. *J. Neurosci. Res.* **1998**, *51*, 293–308.
(22) Mattson, M. P.; Cheng, B.; Davis, D.; Bryant, K.; Lieberburg, I.; Rydel, R. E. beta-Amyloid peptides destabilize calcium homeostasis and render human cortical neurons vulnerable to excitotoxicity. *J. Neurosci.* **1992**, *12*, 376–389.
(23) Cano-Abad, M. F.; Villarroya, M.; García, A. G.; Gabilán, N. H.; López, M. G. Calcium entry through L-type calcium channels causes mitochondrial disruption and chromaffin cell death. *J. Biol. Chem.* **2001**, *276*, 39695–39704.
(24) Sobrado, M.; López, M. G.; Carceller, F.; García, A. G.; Roda, J. M. Combined nimodipine and citicoline reduce infarct size, attenuate apoptosis, and increase bcl-2 expression after focal cerebral ischemia. *Neuroscience* **2003**, *118*, 107–113.
(25) Fu, H.; Li, W.; Lao, Y.; Luo, J.; Lee, N. T.; Kan, K. K.; Tsang, H. W.; Tsim, K. W.; Pang, Y.; Li, Z.; Chang, D. C.; Li, M.; Han, Y. Bis(7)-tacrine attenuates beta amyloid-induced neuronal apoptosis by regulating L-type calcium channels. *J. Neurochem.* **2006**, *98*, 1400–1410.
(26) Perry, G.; Cash, A. D.; Smith, M. A. Alzheimer' s disease and oxidative stress. *J. Biomed. Biotechnol.* **2002**, *2*, 120–123.
(27) Tan, D. X.; Manchester, L. C.; Sainz, R.; Mayo, J. C.; Alvares, F. L.; Reiter, R. J. Antioxidant strategies in protection against neurodegenerative disorders. *Expert Opin. Ther. Pat.* **2003**, *13*, 1513–1543.
(28) Klatte, E. T.; Scharre, D. W.; Nagaraja, H. N.; Davis, R. A.; Beversdorf, D. Q. Combination therapy of donepezil and vitamin E in Alzheimer's disease. *Alzheimer Dis. Assoc. Disord.* **2003**, *17*, 113–116.
(29) Marco-Contelles, J.; León, R.; de Los Ríos, C.; Guglietta, A.; Terencio, J.; López, M. G.; García, A. G.; Villarroya, M. Novel multipotent tacrine−dihydropyridine hybrids with improved acetylcholinesterase inhibitory and neuroprotective activities as potential drugs for the treatment of Alzheimer's disease. *J. Med. Chem.* **2006**, *49*, 7607–7610.
(30) Schwyzer, A.; Cruikshanks, G. S. Reaction products of ethyl benzalacetoacetate an cyclic ketones in the presence of secondary bases or sodium etylate. *J. Prakt. Chem.* **1914**, *89*, 189–193.
(31) Fey, P.; Angerbauer, R.; Huebsch, W.; Bischoff, H.; Petzinna, D.; Schmidt, D.; Thomas, G. Preparation of pyrimidinyldihydroxyalakanoates as antihypercholesterolemics. Patent EP 330057, 1989.
(32) Meyer, H.; Bossert, F.; Vater, W.; Stoepel, K. Dialkyl 4-aryl-2,6-dimethyl-1,4-dihydro-3,5-pyridinecarboxylates. Patent DE 2117572, 1972.
(33) Loudon, J. D.; Tennant, G. Substituent interactions in ortho-substituted nitrobenzenes. *J. Chem. Soc.* **1962**, 3092–3097.
(34) Edwards, J. D.; Pianka, M. Fungitoxicity. IV. Fungitocixity of certain ethylenic compounds. *J. Sci. Food Agric.* **1992**, *14*, 55–58.
(35) Heller, G.; Lauth, H.; Buchwaldt, A. Reactivity of the nitrobenzaldehydes. *Chem. Ber.* **1922**, *55B*, 483–489.
(36) Silver, R. F.; Kerr, K.; Frandsen, P. D.; Kelley, S. J.; Holmes, H. L. Synthesis and chemical reactions of some conjugated heteroenoid compounds. *Can. J. Chem.* **1967**, *9*, 45.
(37) Baltzly, R. The preparation and properties of a platinized charcoal catalyst with some observations on the behaviour of inhibitors. *J. Am. Chem. Soc.* **1952**, *74*, 4586–4589.
(38) Marvel, C. S.; Stille, J. K. Preparation of the pyridalacetones and the inductive effect of nitrogen on the degradation of the intermediate aldols. *J. Org. Chem.* **1957**, *22*, 1451–1457.
(39) Troschütz, R.; Dennstedt, T. Synthese von substituierten 2-Aminonicotinonitrilen. *Arch. Pharm.* **1994**, *327*, 33–40.
(40) McElvain, S. M.; Schoeder, J. P. Orthoesters and related compounds from malono- and succinonitriles. *J. Am. Chem. Soc.* **1949**, *71*, 40–46.
(41) Troschütz, R. Synthesis of pyrido[2,3-*d*]pyrimidines with a trimethoprom partial structure. *Arch. Pharm.* **1989**, *322*, 285–290.
(42) Cheng, C. C.; Yan, S. J. The Friedländer synthesis of quinolines. *Org. React.* **1982**, *28*, 37–201.
(43) León, R.; Marco-Contelles, J.; García, A. G.; Villarroya, M. Synthesis, acetylcholinesterase inhibition and neuroprotective activity of new tacrine analogues. *Bioorg. Med. Chem.* **2005**, *13*, 1167–1175.
(44) Rappaport, F.; Fischl, J.; Pinto, N. An improved method for the estimation of cholinesterase activity in serum. *Clin. Chim. Acta* **1959**, *4*, 227–230.
(45) Ellman, G. L.; Courtney, K. D.; Andres, B. J.; Featherstone, R. M. A new and rapid colorimetric determination of acetylcholinesterase activity. *Biochem. Pharmacol.* **1961**, *7*, 88–95.
(46) Cousins, M. S.; Carriero, D. L.; Salamone, J. D. Tremulous jaw movements induced by the acetylcholinesterase inhibitor tacrine: effects of antiparkinsonian drugs. *Eur. J. Pharmacol.* **1997**, *322*, 137–145.
(47) Piazzi, L.; Rampa, A.; Bisi, A.; Gobbi, S.; Belluti, F.; Cavalli, A.; Bartolini, M.; Andrisano, V.; Valenti, P.; Recanatini, M. 3-(4-{[Benzyl(methyl)amino]methyl}phenyl)-6,7-dimethoxy-2*H*-2-chromenone (AP2238) Inhibits Both Acetylcholinesterase and Acetylcholinesterase-Induced β-Amyloid Aggregation: A Dual Function Lead for Alzheimer's Disease Therapy. *J. Med. Chem.* **2003**, *46*, 2279–2282.
(48) Harel, M.; Schalk, I.; Ehret-Sabatier, L.; Bouet, F.; Goeldner, M.; Hirth, C.; Axelsen, P. H.; Silman, I.; Sussman, J. L. Quaternary ligand binding to aromatic residues in the active-site gorge of acetylcholinesterase. *Proc. Natl. Acad. Sci. U.S.A.* **1993**, *90*, 9031–9035.

(49) Bourne, Y.; Taylor, P.; Radic, Z.; Marchot, P. Structural insights into ligand interactions at the acetylcholinesterase peripheral anionic site. *EMBO J.* **2003**, *22*, 1–12.
(50) Bourne, Y.; Kolb, H. C.; Radic, Z.; Sharpless, B.; Taylor, P.; Marchit, P. Freeze-frame inhibitor captures acetylcholinesterase in a unique conformation. *Proc. Natl. Acad. Sci. U.S.A.* **2004**, *101*, 1449–1454.
(51) Harel, M.; Sonoda, L. K.; Silman, I.; Sussman, J. L.; Rosenberry, T. Crystal structure of thioflavin T bound to the peripheral site of *Torpedo californica* acetylcholinesterase reveals how thioflavin T acts as a sensitive fluorescent reporter of ligand binding to the acylation site. *J. Am. Chem. Soc.* **2008**, *130*, 7856–7861.
(52) Senapati, S.; Bui, J. M.; McCammon, J. A. Induced fit in mouse acetylcholinesterase upon binding a femtomolar inhibitor: A molecular dynamics study. *J. Med. Chem.* **2005**, *48*, 8155–8162.
(53) Mũoz-Ruiz, P.; Rubio, L.; Garc'a-Palomero, E.; Dorronsoro, I.; del Monte-Millń, M.; Valenzuela, R.; Usń, P.; de Austria, C.; Bartolini, M.; Andrisano, V.; Bidon-Chanal, A.; Orozco, M.; Luque, F. J.; Medina, M.; Martínez, A. Design, synthesis, and biological evaluation of dual binding site acetylcholinesterase inhibitors: New disease-modifying agents for Alzheimer's disease. *J. Med. Chem.* **2005**, *48*, 7223–7233.
(54) Marco, J. L.; de los Ríos, C.; García, A. C.; Villarroya, M.; Carreiras, M. C.; Martins, C.; Eleutério, A.; Morreale, A.; Orozco, M.; Luque, F. J. Synthesis, biological evaluation and molecular modelling of diversely functionalized heterocyclic derivatives as inhibitors of acetylcholinesterase/butyrylcholinesterase and modulators of Ca^{2+} channels and nicotinic receptors. *Bioorg. Med. Chem.* **2004**, *12*, 2199–2218.
(55) Maroto, R.; De la Fuente, M. T.; Artalejo, A. R.; Abad, F.; López, M. G.; García-Sancho, J.; García, A. G. Effects of Ca^{2+} channel antagonists on chromaffin cell death and cytosolic Ca^{2+} oscillations induced by veratridine. *Eur. J. Pharmacol.* **1994**, *270*, 331–339.
(56) Di, L.; Kerns, E. H.; Fan, K.; McConnell, O. J.; Carter, G. T. High throughput artificial membrane permeability assay for blood−brain barrier. *Eur. J. Med. Chem.* **2003**, *38*, 223–232.
(57) Reviriego, F.; Rodríguez-Franco, M. I.; Navarro, P.; García-España, E.; Liu-González, M.; Verdejo, B.; Domènech, A. The sodium salt of diethyl 1*H*-pyrazole-3,5-dicarboxylate as an efficient amphiphilic receptor for dopamine and amphetamines. Crystal structure and solution studies. *J. Am. Chem. Soc.* **2006**, *128*, 16458–16459.
(58) Pavón, F. J.; Hernández-Folgado, L.; Bilbao, A.; Cippitelli, A.; Jagerovic, N.; Abellán, G.; Rodríguez-Franco, M. I.; Serrano, A.; Macías, M.; Navarro, M.; Goya, P.; Rodríguez de Fonseca, F. Antiobesity effects of the novel in vivo neutral cannabinoid receptor antagonist 5-(4-chlorophenyl)-1-(2,4-dichlorophenyl)-3-hexyl-1H-1,2,4-triazole−LH 21. *Neuropharmacology* **2006**, *51*, 358–366.
(59) Racemic *p*-methoxytacripyrine **11** has been resolved by chiral HPLC-semipreparative chromatography. Enantiomer (**A**)-**11** $\{\alpha\]_D^{25}$ +179 (*c* 0.5, $CHCl_3$)} and enantiomer (**B**)-**11** $\{[\alpha]_D^{25}$−180 (*c* 0.62, $CHCl_3$)} showed AChE/BuChE inhibition values [(**A**)-**11**: (IC_{50} EeAChE = 80 ± 12 nM; IC_{50} hAChE = 378 ± 40 nM; IC_{50} hBuChE = 11000 ± 2000 μM); (**B**)-**11**: (IC_{50} EeAChE = 9 ± 1 nM; IC_{50} hAChE = 36 ± 3 nM; IC_{50} hBuChE = >100000)] (Supporting Information), in good agreement with the predictions of the molecular modeling. The assignment of the absolute configuration at the stereogenic center, the X-ray analysis of one or both enantiomers of compound **11** with AChE, as well as some biological tests in vivo on each enantiomer, are now in progress and will be reported here in due course.

JM801292B